Published in final edited form as:
Dev Biol. 2014 September 1; 393(1): 93–108. doi:10.1016/j.ydbio.2014.06.016.

The Novel Smad Protein Expansion Regulates Receptor Tyrosine Kinase Pathway to Control *Drosophila* Tracheal Tube Size

Ekaterini Iordanou, **Rachana R. Chandran**, **Yonghua Yang**, **Mina Essak**, **Nicholas Blackstone**, and **Lan Jiang***
Department of Biological Sciences Oakland University Rochester, MI 48309

Abstract

Tubes with distinct shapes and sizes are critical for the proper function of many tubular organs. Here we describe a unique phenotype caused by the loss of a novel, evolutionarily-conserved, *Drosophila* Smad-like protein, Expansion. In *expansion* mutants, unicellular and intracellular tracheal branches develop bubble-like cysts with enlarged apical membranes. Cysts in unicellular tubes are enlargements of the apical lumen, whereas cysts in intracellular tubes are cytoplasmic vacuole-like compartments. The cyst phenotype in *expansion* mutants is similar to, but weaker than, that observed in double mutants of *Drosophila* type III receptor tyrosine phosphatases (RPTPs), Ptp4E and Ptp10D. Ptp4E and Ptp10D negatively regulate the receptor tyrosine kinase (RTK) pathways, especially epithelial growth factor receptor (EGFR) and fibroblast growth factor receptor/breathless (FGFR, Btl) signaling to maintain the proper size of unicellular and intracellular tubes. We show Exp genetically interacts with RTK signaling, the downstream targets of RPTPs. Cyst size and number in *expansion* mutants is enhanced by increased RTK signaling and suppressed by reduced RTK signaling. Genetic interaction studies strongly suggest that Exp negatively regulates RTK (EGFR, Btl) signaling to ensure proper tube sizes. Smad proteins generally function as intermediate components of the transforming growth factor-β (TGF-β, DPP) signaling pathway. However, no obvious genetic interaction between *expansion* and TGF-β (DPP) signaling was observed. Therefore, Expansion does not function as a typical Smad protein. The *expansion* phenotype demonstrates a novel role for Smad-like proteins in epithelial tube formation.

Keywords

Expansion; Smad; RTK; Map kinase; Rho; tracheal; cyst

*Author for correspondence: Dodge Hall of Engineering 322 2200 N. Squirrel Road Rochester, MI, 48309 Jiang23@oakland.edu Tel: (248) 3703552 Fax: (248) 3704225 .

INTRODUCTION

Branched tubular organs such as the lung, vascular system, and kidney are essential for transporting oxygen, nutrients, and cells in all multicellular organisms. The optimal flow of transported fluids depends on the uniform length and diameter of the tubes. Aberrant tube sizes that arise during development lead to devastating human illnesses, such as polycystic kidney disease and blood vessel stenosis (Lubarsky and Krasnow. 2003). While the early patterning and branching of tubular networks have been studied extensively in several systems (Horowitz and Simons. 2008; Lu and Werb. 2008; Andrew and Ewald. 2010), the cellular and molecular mechanisms of tube-size regulation remain poorly understood.

The *Drosophila* trachea is a ramifying network of epithelial tubes with the apical surfaces facing the lumen and the basal surfaces facing surrounding tissues. The fully developed trachea consists of four types of tubes that differ in sizes and architecture (Samakovlis, et al. 1996). Type I tubes are multicellular, such as the dorsal trunk (DT) and the majority of transverse connective (TC). In these tubes, several cells are connected by intercellular junctions and surround an extracellular central lumen. The narrower Type II tubes are unicelluar, such as the lateral trunk (LT), ganglionic branch (GB), dorsal branch (DB), and visceral branch (VB). These tubes are comprised of a linear arrangement of single cells whose apical surfaces surround an extracellular lumen. Cells of unicellular tubes connect themselves around the lumen with autocellular junctions. Type III tubes are intracellular tubes to connect neighboring branches. In these tubes, two donut shaped cells arrange in a linear head-to-tail configuration, and their apical surfaces span the inner wall of the donut, resulting in seamless tubes without intracellular junctions. Type IV tubes are highly branched intracellular cytoplasmic extensions that form in terminal cells at the tips of the unicellular tubes, such as lateral ganglionic branch (LG).

Tracheal tube size is tightly linked to branch identity, and each tube has a distinct width and length. The specification of tracheal tubes initially depends on signaling pathways, including the Epidermal Growth Factor (EGF; Spitz), Transforming Growth Factor-β (TGF-β; Decapentaplegic), and Wingless (Wg) pathways (Chen, et al. 1998; Llimargas and Casanova. 1999). This initial specification is followed by Fibroblast Growth Factor (FGF; Branchless) signaling, which directs the migration of tracheal cells in stereotypical directions to form distinct branches. Once branches are formed, tube size is modified by changes along the apical side of the tracheal cells (Beitel and Krasnow. 2000).

The chitin-based apical luminal matrix, cell junctions, apical secretion, as well as endocytosis have been implicated in tube-size regulation. Mutations disrupting chitin biosynthesis (*krotzkopf verkehrt* and *mummy/cystic*) and matrix assembly (*knickkopf* and *retroactive*) grow over-dilated tubes (Araujo, et al. 2005; Devine, et al. 2005; Moussian, et al. 2006). In contrast, mutations affecting chitin modification (*vermiform* and *serpentine*) (Luschnig, et al. 2006) and septate junctions (SJ, analogous to vertebrate tight junctions) lead to longer tubes (Behr, et al. 2003; Paul, et al. 2003; Llimargas, et al. 2004; Wu, et al. 2004; Luschnig, et al. 2006; Moyer and Jacobs. 2008; Laprise, et al. 2010). In addition, defects in the general apical secretion pathway cause narrower tubes (Jayaram, et al. 2008; Norum, et al. 2010), whereas loss of function mutations in the endocytosis pathway show

over-dilated tubes (Behr, et al. 2007). Current knowledge in mechanisms of tube size regulation discussed above is mostly revealed in multicellular dorsal trunk studies.

Literature on terminal branch (intracellular tube) morphology and size control has recently grown rapidly. Terminal branch development contains five major morphogenesis and maturation steps: branching, growth, tubulogenesis, gas-filling, and maintenance. A systematic screen revealed that cytoskeletal and secretory pathways play important roles in terminal branch morphogenesis (Ghabrial, et al. 2011). For example, both Whacked and Rab35-mediated minus-end directed transport of apical membrane, as well as exocyst-mediated membrane trafficking are required for seamless tube outgrowth (Schottenfeld-Roames and Ghabrial. 2012; Jones, et al. 2014). Loss of function of *wheezy*, which encodes a germinal center kinase, results in terminal branch over-dilation, partially through enriched Rab11-mediated trafficking of the apical membrane protein Crumbs (Song, et al. 2013). Different types of tubes might employ some similar mechanisms to regulate tube size; however, as tube structures vary, branch-specific mechanisms likely exist.

In this paper, we describe the role of *Drosophila* Expansion (Exp, CG13188), a novel Smad-like protein in tube-size regulation. *exp* mutants develop bubble-like cysts in unicellular and intracellular, but not multicellular tubes, suggesting that *exp* is required for branch specific tubesize regulation. Smad proteins are generally known as intracellular mediators of TGF-β signaling (Shi. 2001). TGF-β signaling controls cranial vessel size in zebrafish by regulating cell number (Roman, et al. 2002), and it also regulates *Drosophila* tracheal branch specification and migration (Chen, et al. 1998). However, both branch identity and cell number were not changed in *exp* mutants. In addition, the loss or gain of function in *Drosophila* TGF-β signaling mutants have no obvious tube-size defects (Chen, et al. 1998; Myat, et al. 2005). Therefore, *exp* may not function as a mediator of TGF-β signaling like a typical Smad. Interestingly, the unique *exp* phenotype has not been discovered in any genetic screens for tube-size defects. A similar phenotype was only discovered in double mutants of Type III receptor protein tyrosine phosphatases (RPTPs), *Ptp4EPtp10D* (Jeon, et al. 2008). These are the only two Type III RPTPs in *Drosophila* (Jeon, et al. 2008).

Studies have suggested that Type III RPTPs are negative regulators of the receptor tyrosine kinases (RTKs) that work by dephosphorylating the RTKs and their substrates (Tonks. 2006; Matozaki, et al. 2010). Upon ligand binding and phosphorylation, the kinase activity of RTK phosphorylates downstream effectors to transmit signals. In the *Drosophila* trachea, these are found as: EGFR (epidermal growth factor receptor), Btl (fibroblast growth factor receptor ortholog Breathless), and Pvr [the platelet-derived growth factor receptor (PDGFR)/vascular-endothelial growth factor receptor (VEGFR)/colony stimulating factor 1 (CSF1R)] (Glazer and Shilo. 1991; Cho, et al. 2002; Cela and Llimargas. 2006). MAP kinase and Rho pathways are the two well-known downstream pathways of RTKs (Brand and Perrimon. 1994; Schiller. 2006). Genetic interaction studies suggest that overactive RTKs (especially EGFR and Btl), and the downstream MAP kinase and Rho pathways, contribute to the cyst phenotype observed in *Ptp4EPtp10D* double mutants in the *Drosophila* trachea (Jeon and Zinn. 2009; Jeon, et al. 2012).

To test the idea that Exp regulates tube size using a similar mechanism as RPTPs, we examined genetic interactions between Exp and components of the RTK signaling pathways (EGFR, Btl, MAP kinase, and Rho GTPase). We decreased or increased RTK signaling by expressing dominant negative (DN) and constitutively active (CA) constructs of these components in the trachea in an *exp* mutant background, and then analyzed their effects on the cyst phenotype. Activating RTK signaling enhanced the cyst phenotype in *exp* mutants whereas inhibiting RTK signaling reduced the cyst phenotype. Our results strongly suggest that Exp functions as a negative regulator of RTK signaling to control tube size in unicellular and intracellular branches. The functional analysis of this novel Smad protein reveals a previously unidentified role for Smad family proteins in regulating RTK signaling to control epithelial tube formation.

MATERIAL AND METHODS

Drosophila strains

We used w^{1118} as the wild-type control strain. To generate *exp* mutants, 100 *y w;* $EP[PI31^{G7971}]$ virgin females were crossed to 100 jump starter *y w;* $P[w^{+};\ \Delta 2\text{-}3]$ males. Resulting F1 *w;* $EP[PI31^{G7971}]/\ P[w^{+};\ \Delta 2\text{-}3]$ males (200) were crossed to *y w; Pin/CyO* virgin females (200). Individual white-eyed males from the F2 generation (400) were selected and backcrossed to *y w; Pin/CyO* $P[w^{+};\ twi\text{–}GFP]$ females to establish stocks. We tested 400 jump-out lines for failure to complement *Df(2R)BSC879* [48C5-48E2], which is deleted for *exp* [48D3-D5]. We sequenced genomic DNA PCR amplified from mutant alleles to determine the deletion breakpoints. Two *exp* null mutant alleles were isolated: exp^{135} and exp^{11}. Homozygous mutant individuals were identified in genetic experiments by the absence of *GFP* expression from *CyO* $P[w^{+};\ twi\text{–}GFP]$. The following *Drosophila* strains were also used: *y w;* $P[w^{+};\ btl\text{-}Gal4]$ (Klambt, et al. 1992) to drive various tracheal specific UAS expression. The following *Drosophila* stocks were obtained from the Bloomington Stock Center: *UAS-*$Egfr^{Elp}$, *UAS-Egfr-DN*, *UAS-PhI-CA*, *UAS-Rho1V14*, *UAS-Rho1N19*, *UAS-Rac1V12*, *UAS-Rac1N17*, *UASCdc42V12*, *UAS-Cdc42N17*, $punt^{135}$. *UAS-λBtl*, *UAS-Btl-DN*, *btl-Gal4* were provided by M. Krasnow (Stanford University, Stanford, CA, USA), and *UAS-TKVQ253D* was provided by MM. Myat (Weill Cornell Medical College, NY, USA). $Ptp4E^{1}Ptp10D^{1}$*/FM7-GFP;Btl-Gal4* line was provided by K. Zinn (California Institute of Technology, CA, USA).

Generation of *expansion* cDNA clones

Total RNA from an overnight collection of *Drosophila* embryos was extracted using an RNAeasy Mini Kit (Qiagen). Poly(A)$^{+}$ mRNA was extracted from total RNA using Oligotex (Qiagen). First-strand cDNA was synthesized using SuperScript reverse transcriptase (Gibco-BRL) and used as a template for PCR. Two pairs of primers predicted to cover the cDNA of *exp* isoforms A and B were utilized: (A Forward: 5′-ATGGTGTCGCGTCGAAAAATTCTATCACG-3′ and A Reverse: 5′-TTAGTAGTCGAGTATTTGGATTTTCTTCAGGCTG-3′; B Forward: 5′-ATGGTGTCGCGTCGAAAAATTCTATCACG-3′ and B Reverse: 5′-TCAGTCCCATTCCCCGATGAA-3′). *exp-A* encodes a fragment of 3078 bp, and *exp-B*

codes a fragment of 1542 bp. The amplified fragments were cloned into pCR2.1 (Invitrogen) and sequenced.

Generation of *UAS* HA-tagged *exp* transgenic strains

To generate HA-tagged *exp* fragments, *exp-A* and *exp-B* cDNA fragments without the ATG start codon were PCR amplified and cloned into pCR8/GW/TOPO (Invitrogen). The inserts were then cloned into pAHW, a HA-tag-containing Gateway compatible vector (http://www.ciwemb.edu/labs/murphy), using Gateway LR Clonase II plus (Invitrogen). *HA-exp-A* and *HA-exp-B* were then PCR-amplified and cloned into pCR8/GW/TOPO. The following primers were used: *HA-exp-A* Forward: 5′-GTGTCGCGTCGAAAAATTCTATCACG-3′ and A Reverse: 5′-TTAGTAGTCGAGTATTTGGATTTTCTTCAGGCTG-3′ *HA-exp-B* Forward: 5′-GTGTCGCGTCGAAAAATTCTATCACG-3′ and B Reverse: 5′-TCAGTCCCATTCCCCGATGAA-3′. Inserts were then cloned into the P element vector pT (http://www.ciwemb.edu/labs/murphy), a *Drosophila* Gateway-compatible vector that carries an upstream UAS sequence, using Gateway LR Clonase II. The *UAS-HA-exp* transgenes were introduced into the *Drosophila* germline by microinjection.

Drosophila in situ hybridization

Drosophila whole-mount embryos were hybridized *in situ* to a *Drosophila exp* antisense RNA probe. The probes that recognize both *exp* isoforms or only the *exp-A* isoform were generated by PCR amplification of the *exp* cDNA fragments. The PCR product was cloned into PCRII-TOPO, and the digoxigenin (DIG)-labeled RNA probes were synthesized using SP6 RNA polymerase (Promega) at 37 °C for 3 hr. The probe was added to the hybridization buffer [50% deionized formamide, 5xSSC (1xSSC is 0.15 M NaCl plus 0.015 M sodium citrate), 100 μg/ml of sonicated, denatured salmon sperm DNA, 100 μg/ml of *E. coli* tRNA, 50 μg/ml of heparin, 0.1% Tween 20, pH 4.5]. Hybridization was carried out for 16 hr at 55 °C. After a washing step, hybridized embryos were blocked in 0.5% blocking buffer (Perkin Elmer) and incubated in anti-dig-POD antibody (Roche) diluted 1:50 in 0.5% blocking buffer for 1 hr. Following three 10 min PT (PBS, 0.1% Tween-20) washes, embryos were incubated for 1 hr in TSA-Cy3 diluted in amplification diluent (Perkin Elmer). TSA reactions were stopped by three 5 min PT washes. Embryos were mounted in 70% glycerol and examined by confocal microscopy.

Exp antibody production

Polyclonal antibodies against Exp were generated by using an Exp fusion protein containing an N-terminal His_6-tag. An *exp* fragment corresponding to amino acids (aa) 233-477 of *exp-B* was PCR amplified using the primers: 5′-CTCGAGAAGAGCAAACTGCCACCAGTG-3′ and 5′-CTCGAGGTCCCATTCCCCGATGAACATG-3′ (the XhoI restriction sites are underlined), then digested with XhoI, and cloned into the XhoI site of pET-16b (Novagen). After transformation into *Escherichia coli* BL21(DE3), cells were grown and His_6-Exp fusion protein synthesis was induced by addition of IPTG (isopropyl-β-d-thiogalactopyranoside). Inclusion bodies were prepared, solubilized in 10% sodium dodecyl sulfate (SDS), dialyzed in 0.05% SDS, 1 mM phenylmethylsulfonyl fluoride, PBS, and purified using a Talon metal

affinity resin (Clontech). The eluted His_6-Exp protein was then dialyzed in 0.01% SDS, PBS. Two guinea pigs were immunized by subcutaneous injection of protein (Pocono Rabbit Farm & Laboratory).

Western Blot

To prepare protein extracts, 50 *Drosophila* embryos of wild type w^{1118} and exp^{135} between S14-S17 were homogenized and treated with 50 μl protein extraction lysate buffer (1M Tris pH 8.2, 5M NaCl, 10% SDS, 10% SDC, 100% NP40, 100 mM PMSF, protease inhibitor) respectively. The homogenate was centrifuged at 15,000 g for 5 min at 4 °C, and the supernatant was further centrifuged with glycerol at 15,000 g for 5 min at 4 °C to precipitate the crude membrane fraction. Protein concentration of the supernatant was then measured using the Coomassie assay. Cell lysates were heated to 100 °C, an SDS sample buffer was added, and the lysates were separated on an 8% gel by SDS-PAGE, transferred to a polyvinylidene difluoride membrane, and subjected to immunoblotting with anti-Exp (1:1000 dilution). Next, the same membrane was washed with stripping buffer and subjected to immunobloting with anti-β-actin. The immunoblot was developed with Western Lightning reagents (Perkin Elmer) according to the manufacturer's recommendation.

Drosophila immunostaining

Whole-mount embryos were immunostained as described previously (Patel, et al. 1987). The following primary antibodies and dilutions were used for immunostaining: anti-Exp (Guinea Pig 1:200), anti-Trh (rat 1:100) (Ward, et al. 1998), anti-GFP (chicken 1:500, Abcam), anti-RFP (rabbit 1:500, Abcam), anti-Crumbs (mouse 1:100, DSHB), MAb 2A12 (mouse IgM 1:5, DSHB), anti-DE-Cadherin (rat 1:3, DSHB), anti-Coracle (Guinea Pig 1:2000) (Lamb, et al. 1998), anti-Verm (Rabbit 1:100) (Luschnig, et al. 2006), anti-Rip11 (rabbit 1:100) (Li, et al. 2007), anti-uninflatable (Uif) (Guinea Pig 1:100) (Zhang and Ward. 2009), anti-HA (rabbit 1:100, Invitrogen). The following secondary antibodies were used: (1) AlexaFluor 594 anti-mouse IgM, (2) AlexaFluor 543 anti-Rat IgG, anti-Rabbit IgG, anti-Guinea Pig IgG, (3) AlexaFluor 488 anti-Rat IgG, anti-rabbit IgG, and anti-Guinea Pig IgG, (4) AlexaFluor 647 anti-Rat IgG, anti-Rabbit IgG, and anti-Guinea Pig IgG (Invitrogen). All secondary antibodies were used at 1:200. Chitin-binding probe was used at 1:50 (New England Biolabs). Photomicrographs were taken with a Nikon Eclipse Ti confocal microscope.

RNAi

Double-stranded RNA (dsRNA) for RNA interference (RNAi) experiments was prepared for *exp* using the same protocol as described earlier (Jiang and Crews. 2003). The templates used for synthesis of dsRNA were the products of two-step PCR. The first step amplified a fragment of cDNA that contains a partial T7 RNA polymerase promoter site. The second PCR step amplified the fragment and completed the addition of a T7 RNA polymerase site adjacent to both ends of the cDNA sequence. The first PCR used to amplify *exp* cDNA utilized the following primer pair: 5′-CGACTCACTATAGGG CTCGAGAAGAGCAAACTGCCACCAGTG-3′ and 5′-CGACTCACTATAGGG CTCGAGGTCCCATTCCCCGATGAACATG -3′ (the T7 sequences are underlined). This

fragment is the same as the fragment used to generate Exp antibody. The second step of the PCR used the T7 promoter sequence (ATAGAATTCTCTAGAAGCTTAATACGACTCACTATAGGG) as a primer. This resulted in an amplified fragment with T7 RNA polymerase sites at both ends, allowing the simultaneous synthesis of sense and antisense RNA. DNA templates were purified by using QIAquick PCR purification kit (Qiagen). dsRNAs were synthesized by using T7 RNA polymerase and DNA templates were removed with RNase-free DNase. After phenol-chloroform extraction and ethanol precipitation, the dsRNAs were dissolved in Tris-EDTA (TE) at a final concentration of 5 μM. Analysis of dsRNAs by agarose gel electrophoresis indicated that bands of the expected sizes were present.

Quantification of cyst phenotypes

Stage 16 embryos were stained with anti-Crumbs or anti-Uninflatable to outline the apical membrane. Samples were imaged using Nikon confocal microscopy and *z*-stack projections were obtained. Measurements were made using the Nikon NLS Elements program. Comparison of tracheal metameres (Tr5-8) from mutant embryos showed little variation between hemisegments and thus measurements for all four hemisegments were pooled; ~ 10 embryos were scored per genotype. All spherical enlargements along LT and GB were counted as cysts and diameters were measured. For controls without LT and GB cysts, two measurements were made at the thickest points of each LT and GB branch.

RESULTS

Identification of the *Drosophila expansion* gene

To identify novel genes required for tube-size regulation, we performed an RNAi knock down screen of ten novel tracheal expressed genes according to the Berkeley *Drosophila* Genome Project (BDGP) gene expression database (http://insitu.fruitfly.org/cgi-bin/ex/insitu.pl). One of these genes, which we named *exp* (*CG13188*), is required for tube-size regulation. Knocking down *exp* by RNAi leads to bubble-like cysts (Fig. 1B, B') with an enlarged diameter in the trachea compared to wild type control (Fig. 1A, A'). The *exp* gene resides at 48D3-D5 on chromosome 2 and produces transcripts that encode two protein isoforms: Exp-A (1025 aa) and Exp-B (513 aa) (Fig. 2A). Transcripts corresponding to the two isoforms were confirmed by RTPCR and sequencing. Analysis of the protein sequence indicates that Exp is a Smad-like protein containing a Mad-homology 2 (MH2) domain (Fig. 2A). Smad proteins are 400-500 amino acids in length, with particularly high similarity in the N-terminal MH1 (Mad-homology 1) domain and the C-terminal MH2 domain (Heldin, et al. 1997). The MH2 domain is responsible for interacting with other proteins, whereas the MH1 domain exhibits sequence-specific DNA binding. Generally, Smads are intracellular mediators of the TGF-β signaling pathway (Shi. 2001). Smads that contain only the MH2 domain, such as the daughters against DPP (Dad) protein, function as regulators of TGF-β signaling (Tsuneizumi, et al. 1997). Exp contains only an MH2 domain, but no MH1 domain, indicating that it may potentially act as a regulator of the TGF-β signaling pathway. However, it is also possible that Exp does not act as a typical Smad protein and regulates tube size through other signaling pathways or cellular processes. Phylogenetic analysis of the MH2 domain of Exp shows that it forms a subfamily with *Drosophila* CG13183 (Dro-

CG13183), *Anopheles gambiae* AGAP007416 (An-AGAP007416), and *Caenorhabditis elegans* C34E11.2c (Ce-C34E11.2c). Furthermore, it is distantly related to human proteins Smad2 and BAH12971 (Fig. 2B). Quantitatively, the MH2 region of Exp shows the following percent identity and similarity to the other Exp subfamily proteins: Ano-AGAP007416 91% (identity) and 98% (similarity), Dro-CG13183 63% (identity) and 80% (similarity), Ce-C34E11.2c 39% (identity) and 54% (similarity). In addition, Exp is highly conserved in all twelve *Drosophila* species, other insects, and arthropods.

Exp is localized throughout the cytoplasm in all tracheal cells

To visualize the protein localization of Exp in *Drosophila* embryos, an antibody that recognizes both Exp isoforms was generated. The Exp antisera were prepared against a bacteria-synthesized Exp protein derived from a region of the protein not conserved in other Smad proteins (Fig. 2A). Immunostaining of whole-mount w^{1118} embryos revealed that the Exp protein was localized in all tracheal cells from stage 12 through the end of embryogenesis, stage 17 (Fig. 3B'-G'), but not at the tracheal placode, stage 11 (Fig. 3A'). Staining in epidermal cells was also observed at late stages of embryogenesis, stage 16-17 (arrowheads in Fig. 3F'-G'). The expression pattern of the Exp protein is identical to the *exp* RNA pattern revealed by fluorescence *in situ* hybridization (Fig. 3A-G), suggesting antibody specificity. An *exp* probe that recognizes both isoforms was used (Fig. 2A). The specificity of the Exp antisera was further demonstrated by an absence of Exp staining in *exp* deletion strains (*Df(2R)BSC879 [48C5-48E2])* (Fig. 3H) even though tracheal cells were present (Fig. 3H'). To visualize cellular localization of Exp in the trachea, membrane marker GAP-GFP was expressed in all tracheal cells and nuclei were determined by a tracheal nuclear protein, Trachealess (Trh) (Wilk, et al. 1996). The cellular localization of Exp protein was observed throughout the cytoplasm (Fig. 3I, I") but not in nuclei (asterisks in Fig. 3I"). In addition, partial overlap between Exp and the membrane marker GAP-GFP was also observed (arrowhead in Fig. 3I). These results suggest that Exp functions at the level of the cytoplasm and probably also membrane, but not in the nucleus. Additionally, to reveal possible differential expression patterns of the two Exp isoforms, we performed *in situ* hybridization using *exp-A* probe that specifically recognizes the longer form of *exp* (Fig. 2A). No tracheal staining was detected (Fig. 3K), suggesting that the *exp-A* isoform is expressed at a very low level below detection by *in situ*. Consistent with this, the expected 138KD Exp-A was not detected in embryonic protein extracts by Western blot analysis (Fig. 3J). We only detected Exp-B protein (~69 KD) in wild type embryos but not in *exp* null mutant embryos (Fig. 3J). Therefore, the Exp-B isoform is the form expressed in tracheal cells.

Generation of *exp* null mutants

To perform functional analysis of *exp* in tracheal tube-size regulation, we generated *exp* null mutants. The P-element insertion $EP[PI31^{G7971}]$ resides within the *PI31* gene, which is located 3′ downstream of *exp*. Mutants were generated by imprecise excision of the P-element. The exp^{135} excision mutant (Fig. 4A) removed exons 3-11 of the *exp* gene and potentially generates a severely truncated protein (39 aa) that lacks the entire MH2 and C-terminal domains (Fig. 2A). Moreover, this deletion also partially deletes the neighboring *PI31* gene. The exp^{11} mutant (Fig. 4A) removed the entire coding sequence of *exp* (exons

2-11) and also deleted the two neighboring genes, *PI31* and *CG8290*. Another excision deletion, Δ*1*, removed both *PI31* and *CG8290*, while leaving the *exp* locus intact. Immunostaining of mutant embryos revealed that in homozygous exp^{135} (Fig. 4D) and exp^{11} (Fig. 4E) embryos Exp protein was undetectable in tracheal cells (Fig. 4D', 4E'), whereas it was present in Δ*1* mutant embryos, as expected (Fig. 4C). This result suggests that both exp^{135} and exp^{11} are null mutants.

Cysts form on unicellular and intracellular tracheal branches in *exp* mutants

We examined the trachea in wild type and *exp* mutant embryos by staining for an apical membrane marker Crumbs (Crb) (Wodarz, et al. 1995). We observed bubble-like cysts in unicellular (LT, GB) and intracellular (LG) branches, but not in multicellular branches (DT). We also observed bubbles in DB and VB, but to a lesser extent. Therefore, we focused our investigation on branches with a stronger phenotype. In wild type embryos, Crb appeared as a single line in unicellular branches LT and GB (Fig. 1A, A', D). Similar lines were observed in intracellular branches such as LG (Fig. 1D). In homozygous exp^{135} mutant trachea, we observed bubble-like cysts on unicellular LT and GB (Fig. 1C, C', E) as well as intracellular LG (Fig. 1E). However, we did not observe cysts on intracellular fusion branches (Fig. G-G"). Despite the appearance of cysts, the tracheal network of *exp* mutants exhibited normal branching patterns. Consistent with this observation, cysts were also observed in exp^{11}, exp^{135}/exp^{11} and *exp*/*Df(2R)BSC879* mutant embryos (data not shown). The cyst phenotype in *exp* mutants was similar to the defects observed in *exp* RNAi embryos (Fig. 1B, B'). Cysts in *exp* mutants could also be visualized by another apical membrane marker, Uninflatable (Uif), (Zhang and Ward. 2009), which was used interchangeably with Crb to label the apical membrane. To confirm that the cyst phenotype was due to *exp*, as opposed to *PI31*, *CG8920*, or background mutations, we first analyzed the Δ*1* mutant strain, having deleted both *PI31* and *CG8920*. Δ*1* mutants had wild-type-appearing tracheal branches (Supplemental Fig. S1B, B1, B2), and this indicates that the cyst phenotype in *exp* mutants is caused by *exp*, but not other genes. Furthermore, we expressed *HA-exp-B* throughout the trachea using *btl-Gal4* in an *exp* mutant background; it completely rescued the tracheal phenotype in both exp^{135} and exp^{11} mutants (Supplemental Fig. S1C, C1, C2). Thus, *exp* acts autonomously in the trachea to control tube size. We use exp^{135} as the *exp* mutant in the following experiments.

To quantify the cyst phenotype, we counted LT and GB cysts and measured their diameter in 10 embryos (Supplemental Table S2). LT in each exp^{135} mutant tracheal segment contained 2.4±0.2 cysts, with a diameter of 1.7±0.1 μm, whereas the wild type trachea had no cysts and the diameter of the LT was 0.9±0.1 μm, which is consistent with published data (Beitel and Krasnow. 2000). Each GB in exp^{135} had 2.5±0.1 cysts with a diameter of 1.4±0.1 μm, whereas wild type GB had no cysts with a diameter of 0.8 ±0.1 μm.

Unlike cranial vessels in zebrafish, in which tube size is affected by changes in cell number (Roman, et al. 2002), alterations in cell number do not normally play a role in tube-size regulation in the *Drosophila* trachea (Beitel and Krasnow. 2000). To determine whether cell number is involved in the *exp* phenotype, we counted tracheal cell nuclei in tracheal segment 5 (Tr5) (N=10) using anti-Trh staining. There were 80.1±0.5 cells in Tr5 in wild-type

embryos verses 79.5±0.8 in *exp* mutant embryos. Thus, no significant difference was observed between *exp* mutant and wild-type embryos. Therefore, *exp* is not required for the general development of the trachea or tracheal branches, rather it specifically controls cellular processes required for tube-size regulation.

Cysts are modified apical extracellular lumen in unicellular branches and intracellular vacuole-like compartments in intracellular branches

To visualize cyst localization, we expressed membrane localized GFP (mCD8-GFP) driven by *btl-gal4* to mark the cell boundary in the entire trachea. In wild type trachea, the apical membrane marker Crb appeared as a single line in GB (Fig. 5C-C") and intracellular tube LG (Fig. 5E-E") within the cell boundary. Similarly, cysts were also within the cell boundary in both GB (Fig. 5D-D") and LG (Fig. 5F-F") in *exp* mutants. Intracellular tubes are seamless tubes with cytoplasmic extensions in terminal cells. Therefore, the cysts in LG are intracellular vacuole-like compartments.

To characterize cyst composition in unicellular branches, we examined the distribution of apical and basolateral polarity markers. We examined GB and found the apical membrane marker Crb appears as a single line, determining the path of lumen, whereas the basolateral marker Coracle (Cor) outlines the septate junction in wild type control (Fig. 5A-A"'). Similarly, Crb outlined the cysts without overlapping with Cor in *exp* mutants (Fig. 5B-B"'), suggesting cysts are modified apical compartments.

To determine whether the cysts in unicellular tubes are modified apical extracellular lumen or intracellular vacuole-like compartments, we analyzed the association of adherens junctions (AJs) and cysts by staining embryos with the AJ marker Shotgun (Shg; DE-Cadherin), the apical membrane marker Crb, and the tracheal nuclear marker Trh. Unicellular branches are formed by a line of cells with an end-to-end configuration. The apical lumen in unicellular tubes is extracellular and sealed by autocellular AJs (Ribeiro, et al. 2004). In wild type embryos, anti-Shg labeled a single line in GB along the apical membrane outlined by Crb (Fig. 5G-G""). In *exp* mutants, the cysts outlined by Crb were also associated with a single line of Shg that outlines AJs (Fig. 5H-H"'). Almost all cysts we observed were associated with AJs. These observations strongly suggest that cysts in unicellular tubes are modified forms of apical extracellular lumen rather than intracellular vacuole-like compartments.

exp is required for the accumulation of luminal components in unicellular and intracellular branches

To test whether *exp* is required for apical lumen formation, we analyzed the composition of the luminal matrix in *exp* mutants. The tested matrix components include: (1) Gasp (2A12), a chitin binding protein, (2) Piopio, a zona pellucida (ZP) domain protein (required to support migration of cells within the unicellular tube during cell intercalation and cell junction remodeling) (Jazwinska and Affolter. 2004), (3) Verm, a chitin modifying enzyme required to limit tube elongation, and (4) chitin, which forms a transient polysaccharide luminal matrix.

We observed defective accumulation of a subset of luminal components in unicellular and intracellular branches where cysts formed in *exp* mutants. Chitin and Gasp failed to accumulate in the lumen of unicellular and intracellular branches in *exp* mutants (Fig. 6B", B'") compared to control embryos (Fig. 6A", A"'). In contrast to the defective accumulation of Gasp and chitin, the luminal protein Piopio secretion appeared normal in *exp* mutants (Fig. 6B') relative to control embryos (Fig. 6A'). The normal secretion of Piopio was consistent with the correct formation of unicellular tubes through cell intercalation in *exp* mutants (Fig. 5H-H"'). In addition, the secretion of Verm was relatively normal but slightly weaker in LT in *exp* mutant (Fig. 6D) compared to control embryos (Fig. 6C). Despite the accumulation defects of luminal components in unicellular and intracellular branches, the secretion of all luminal components tested, including both 2A12 and chitin, was normal in multicellular branches in *exp* mutants (Fig 6BB"', D). Thus, both cyst and lumen phenotypes are restricted to unicellular tubes and intracellular branches, rather than multicellular branches.

Exp negatively regulates RTK signaling to control tube size

The branch specific cyst phenotype in *exp* mutants is rather unique. It was only observed in the double mutants of type III RPTPs, *Ptp4EPtp10D* (Jeon and Zinn. 2009). Therefore, we speculate Exp regulates tube size using similar mechanisms as RPTPs. We predict two possibilities: (1) Exp is required to maintain RPTP distribution in the trachea; (2) Exp does not directly regulate RPTPs, but their targets. We analyzed Ptp10D distribution in *exp* mutants. Ptp10D was selectively expressed at the apical membrane in both wild type (Fig. 7C-C") and *exp* mutant trachea (Fig. 7D-D"), and no obvious difference was observed. The normal distribution of Ptp10D in *exp* mutants suggests that the *exp* mutant phenotype is likely not caused by the abnormal distribution of RPTPs, since only the *Ptp4EPtp10D* double mutant shows a cyst phenotype.

We then tested the idea that Exp has a similar function to RPTPs to suppress RPTP targets. If that is the case, then Exp overexpression could potentially suppress the cyst phenotype caused by the over activated RPTP targets in *Ptp4EPtp10D* mutants. As expected, when we overexpressed *exp* in the trachea with *btl-Gal4* in a *Ptp4EPtp10D* double mutant background, the cyst phenotype was significantly reduced in LT and GB (Fig. 7B, B1, E) compared to *Ptp4EPtp10D* alone (Fig. 7A, A1). As the number of LG cysts is variable, we qualitatively assessed the effects of *exp* expression on LG bubbles. The diameter of the LG bubble was also reduced (Fig. 7A2, B2). These results suggest that Exp negatively regulates RPTP targets to control tube size.

Type III RPTPs negatively regulate downstream RTK signaling (Matozaki, et al. 2010). Multiple overactive RTK signaling pathway components (EGFR, Btl, Pvr) contribute to cyst formation in *Ptp4EPtp10D* mutants (Jeon, et al. 2012). Among them, EGFR and Btl signaling play more important roles. To further test the idea that Exp downregulates RTK signaling to control tube size, we either increased or decreased EGFR or Btl signaling components in *exp* mutants and analyzed their effects on cyst phenotype. The EGFR-CA transgene carries the Elp mutation, which leads to constitutive receptor activation. The Btl-CA construct was engineered with a lambda receptor dimerization domain in the N-

terminus, which forces ligand-independent dimerization, therefore activating the receptor. The EGFR-DN or Btl-DN constructs significantly reduce or eliminate RTK activity by dimerizing with wild type receptors, forming inactive complexes. When we expressed CA or DN RTK constructs in a wild type background, EGFRCA and Btl-CA caused extra branching, whereas EGFR-DN and Btl-DN led to shorter GBs without generating cyst phenotypes or affecting tracheal branching in general (data not shown). These observations of wild type trachea were consistent with the previous report (Jeon, et al. 2012). We then expressed CA or DN RTK in *exp* mutant trachea and quantitatively analyzed the cyst phenotype in unicellular LT and GB, and qualitatively analyzed cysts in intracellular LG. EGFR-CA in *exp* mutant trachea significantly enhanced cyst phenotype in LT, GB and LG (Fig. 8D, D1, D2, Supplemental Table S2). LT cysts were expanded from 1.7 μm to 2.5 μm (52% increase), GB cysts were expanded from 1.4 μm to 2.5 μm (58% increase). LT cyst number was increased from 2.4 to 3.3, and GB cyst number from 2.5 to 4.0. Similarly, Btl-CA also enhances the cyst phenotype, but to a much lesser extent (Fig. 8F, F1, F2, Supplemental Table S2). Conversely, Btl-DN drastically suppressed the cyst phenotype, reducing cyst number to nearly zero in GB (Fig. 8E, E1, E2, Supplemental Table S2). Likewise, EGFR-DN also considerably rescued the cyst phenotype (Fig. 8C, C1, C2, Supplemental Table S2). Extra branching by EGFR-CA or Btl-CA expression (arrows in Fig. 8D and F) and extension defects in GB by EGFR-DN or Btl-DN expression (Fig. 8C1, E1) were observed in *exp* mutants as in wild type. However, this did not affect analysis of the cyst phenotype. Thus, these genetic interaction assays indicate Exp is a negative regulator of RTK signaling.

Two downstream pathways of RTK signaling, MAP kinase pathway and Rho pathway, are implicated in cyst formation in *Ptp4EPtp10D* double mutants (Jeon, et al. 2012). We expect that these two pathways also contribute to the *exp* phenotype, and we tested their input to the cyst phenotype in GB and LG. Activation of the MAP kinase pathway is mediated by Raf (MAP kinase kinase kinase, MAPKKK) and MEK (MAP kinase kinase, MAPKK), which leads to dual phosphorylation and activation of Erk (MAP kinase, MAPK) (Reich, et al. 1999; Ohshiro, et al. 2002). Raf is a serine/threonine kinase. Expression of activated Raf kinase, called Ph1-CA (Brand and Perrimon. 1994), in the wild type trachea caused extra branching but did not generate any cysts as described earlier (Jeon, et al. 2012). However, it significantly enhanced the cyst phenotype in *exp* mutant trachea in both GB and LG (Fig. 9C, C1, Supplemental Table S2). Extra branching occurred sometimes (arrow in Fig. 9C). This result indicates that the MAP kinase pathway contributes to cyst phenotype in *exp* mutants.

The *Drosophila* Rho family has several components: one Rho, three Rac, and one Cdc42 (Johndrow, et al. 2004). To evaluate the contribution of the Rho pathway to the cyst phenotype, we first expressed CA or DN constructs of Rho pathway components (Rho1, Rac1, Cdc42) in a wild type background. Similar to what was described earlier (Jeon, et al. 2012), Rac1-CA severely disrupted tracheal development; Rho1-CA and Cdc42-CA expression caused fusion defects in DT and LT and extension defects in GB; Rac1-DN caused GB extension defects; Cdc42-DN caused LT fusion defects; Rho1-DN did not cause significant branching defects. However, none of these constructs led to the cyst phenotype

(data not shown). We then expressed these constructs, which did not cause severe trachea developmental defects, in *exp* mutant trachea, and analyzed their effect on the cyst phenotype. Wild type level defects in branching and fusion occurred in *exp* mutants, but this did not limit the observation of cysts. Rho1-CA enhanced cyst phenotype in both GB and LG (Fig. 9D, D1, Supplemental Table S2) whereas Cdc42-CA slightly reduced, rather than enhanced, the cyst phenotype (data not shown). Both Rac1-DN and Rho1-DN partially suppressed the cyst phenotype in GB (Fig. 9E, F, Supplemental Table S2) and in LG (Fig. 9E1, F1, Supplemental Table S2), whereas Cdc42-DN did not have an obvious effect (Fig. 9G, G1, Supplemental Table S2). Therefore, through mainly Rac1 and Rho1, the Rho pathway also contributes to cyst formation in *exp* mutants. Taken together, these genetic interaction assays strongly suggest that Exp downregulates RTK signaling (EGFR, Btl) through two downstream pathways, MAP kinase and Rho, to control tube size.

Exp does not regulate TGF-β signaling to control tube size

Exp is a Smad-like protein containing a MH2 domain, which usually functions as a regulator (such as Dad) of TGF-β (DPP) signaling (Kamiya, et al. 2008). To test the contribution of TGF-β signaling in the *exp* mutant phenotype, we increased or decreased the signaling components in an *exp* mutant background and analyzed their effect on the cyst phenotype. In *Drosophila*, Thick vein (Tkv) and Punt trans-membrane serine-threonine kinase receptors are required in concert to transduce the TGF-β (DPP) signal by phosphorylating Mad. The phosphorylated Mad then binds to the common-mediator Medea and enters the nucleus to regulate target gene expression. Overexpression of a constitutively active form in wild type trachea, Tkv-Q253D, leads to defective DT formation; numerous cells migrate dorsally (Affolter, et al. 1994; Vincent, et al. 1997; Llimargas. 2000). In $punt^{135}$ mutants, all dorsal branches are absent, and GB extension defects are also occasionally observed (Affolter, et al. 1994; Vincent, et al. 1997; Llimargas. 2000). Tkv-Q253D overexpression in *exp* mutant trachea caused defects in DT formation, as expected; however, it did not have any effect on the cyst phenotype in LT, GB, and LG (Fig. 10C, C1, C2). Similarly, despite no DB formation, $punt^{135}$*exp* double mutants showed no obvious changes in cyst phenotype (Fig. 10B, B1, B2).

To further rule out the possibility that Exp functions as a positive or a negative regulator of TGF-β signaling, we expressed *exp* in gain of function or loss of function mutants of TGF-β (DPP) signaling, and then analyzed their effect on branch specific migration defects in these mutants. Constitutively active TGF-β (DPP) signaling in Tkv-Q253D overexpressed embryos have defects in DT formation (Fig. 10E). If Exp negatively regulates TGF-β signaling, then *exp* overexpression likely suppresses this defect. However, we did not observe a reduced DT formation defect (Fig. 10F). In TGF-β (DPP) loss of function mutant $punt^{135}$, all DBs did not form (Fig. 10G). If Exp functions as a positive regulator of TGF-β signaling, overexpression of Exp is expected to suppress the DB migration defect in *punt* mutants. Again, no obvious change was observed (Fig. 10H). Taken together, these results strongly suggest that Exp does not function as a typical Smad protein to mediate TGF-β signaling to control tube size.

DISCUSSION

In this paper, we analyzed the function of Exp, a novel Smad-like protein in tube-size regulation. It is expressed in all tracheal cells, yet the bubble-like cyst phenotype of *exp* mutants was only observed in unicellular and intracellular branches, but not multicellular tubes and fusion tubes. These tubes differ in their shape changes during development and cellular coordination around the lumen. The lumen in unicellular tubes is an extracellular compartment that is sealed by an autocellular junction, whereas lumen in intracellular tubes is a cytoplasmic extension without a cell junction. Fusion tubes are formed by two donut shaped cells connecting neighboring branches. The lumen in multicellular tubes is formed by several cells connected by intercellular junctions. During tracheal development, multicellular branches only increase their size, without dramatic changes in cell shape and the apical membrane. However, unicellular and intracellular branches radically change cell shapes, which require drastic apical membrane expansion. This phenomenon may explain why bubbles are only observed in unicellular and intracellular, but not multicellular tubes.

Unexpectedly, we did not observe bubbles in fusion cells that also undergo significant cell shape changes during branch fusion. The fusion process is a dynamic cellular process involving cell migration, adhesion, vesicle trafficking, cytoskeleton rearrangement, and membrane fusion (Lee and Kolodziej. 2002). We speculate that fusion cell expressed genes may be involved in the regulation of tube size in fusion branches, as occurs with specific genes involved in various aspects of branch fusion. For example, *escargot* and *dysfusion* are involved in the adhesion between two fusion cells, whereas *dead end* regulates intracellular trafficking in lumen formation between two fusion cells (Tanaka-Matakatsu, et al. 1996; Jiang and Crews. 2003; Jiang, et al. 2007). However, genes involved in tube-size regulation of fusion branches have yet to be discovered. Fusion cell expressed genes have been identified, such as CG13196 and CG15252, with their roles in branch fusion remaining to be investigated (Jiang, et al. 2010). These genes may work redundantly with *exp* to further ensure the proper tube size in fusion branches. Therefore, the lack of bubbles in fusion cells of *exp* mutants is likely due to the presence of these genes.

Our results show Exp does not genetically interact with TGF-β signaling to regulate tube size. This result is unexpected because Exp is a Smad-like protein and Smads are well known intracellular mediators of TGF-β signaling (Shi. 2001). TGF-β signaling is implicated in the specification of tracheal branches in *Drosophila* (Chen, et al. 1998) and regulation of cell numbers in cranial vessels of zebrafish (Roman, et al. 2002). Our genetic interaction assays suggest that Exp is neither a positive nor negative regulator of TGF-β signaling. Additionally, TGF-β signaling did not contribute to the cyst phenotype in *exp* mutants. Consistent with this, in *exp* mutant embryos, neither branch identity nor cell number was altered. Thus, this novel Smad does not function as a typical Smad to regulate TGF-β signaling. Rather, our genetic interaction assays strongly suggest that Exp interacts with RTK signaling to control tube size. The strong suppression of the cyst phenotype in *exp* mutants by expressing EGFR-DN and Btl-DN suggests that Exp could negatively regulate these receptors. Exp is cytoplasmic/membrane protein with a MH2 protein interacting domain; therefore, it is possible that Exp directly or indirectly interacts with the cytoplasmic domains of the receptors to regulate their activities. Interestingly, the *Drosophila* protein

interaction database shows Exp as interacting with only one protein, CG11275. In addition, CG11275 interacts with Pointed, Stumps, and Vps36. Stumps and Pointed are components of RTK signaling, whereas Vps36 is involved in protein trafficking at the early endosome (Scholz, et al. 1993; Imam, et al. 1999; Herz, et al. 2009). Therefore, we cannot exclude the possibility that Exp acts on other RTK signaling components, and/or regulates vesicular trafficking to control tube size. It will be interesting to investigate whether the closest *C. elegans* homolog, Ce-c34e11.2c, regulates RTK but not TGF-β signaling, and whether Exp protein interactions are conserved in Ce-c34e11.2c. If Ce-c34e11.2c functions similarly, Exp might define a family of non-TGF-β signaling Smads.

Expression of multiple RTK-CA transgenes could not reproduce the cyst phenotype (Jeon, et al. 2012). This indicates that Exp also regulates other unknown pathways or cellular processes (such as vesicular trafficking) that cooperate with RTK signaling to control tube size. The identification of Exp interacting proteins will further reveal the role of this novel Smad protein in tube-size regulation. Elucidating the function of Exp will provide novel insights into tube-size regulation as well as the role of Smad proteins in general.

CONCLUSION

This work provides a clear understanding of the role of Expansion, a novel Smad protein, in the regulation of *Drosophila* tracheal tube diameter. Exp is required for the restriction of tube dilation in both unicellular and intracellular branches. We used genetic interaction assays to demonstrate that Exp regulates RTK signaling to control tube size. In addition, genetic interaction assays between Exp and TGF-β signaling components strongly suggest that, unlike typical Smad proteins, Exp does not regulate TGF-β signaling to control tracheal tube size. In general, the understanding of tube size regulation is still limited; however, this study provides a significant contribution to this area of research by elucidating a novel mechanism for tube diameter expansion.

Supplementary Material

Refer to Web version on PubMed Central for supplementary material.

Acknowledgments

The authors would like to thank Mark Krasnow, Stephen Luschnig, Rick Fehon, Robert E. Ward, Amin Ghabrial, Steven Wasserman, Monn M. Myat, DSHB, Bloomington *Drosophila* Stock Center, and Vienna *Drosophila* Stock Center for providing *Drosophila* strains. We also thank Joseph McDermott and Stephen Crews for a critical review of the manuscript. This project was supported by National Institutes of Health under Award Number R15GM100369 to Lan Jiang.

REFERENCES

Affolter M, Nellen D, Nussbaumer U, Basler K. Multiple Requirements for the Receptor serine/threonine Kinase Thick Veins Reveal Novel Functions of TGF Beta Homologs during Drosophila Embryogenesis. Development. 1994; 120:3105–3117. [PubMed: 7720555]

Andrew DJ, Ewald AJ. Morphogenesis of Epithelial Tubes: Insights into Tube Formation, Elongation, and Elaboration. Dev Biol. 2010; 341:34–55. [PubMed: 19778532]

Araujo SJ, Aslam H, Tear G, Casanova J. Mummy/cystic Encodes an Enzyme Required for Chitin and Glycan Synthesis, Involved in Trachea, Embryonic Cuticle and CNS Development--Analysis of its Role in Drosophila Tracheal Morphogenesis. Dev Biol. 2005; 288:179–193. [PubMed: 16277981]

Behr M, Wingen C, Wolf C, Schuh R, Hoch M. Wurst is Essential for Airway Clearance and Respiratory-Tube Size Control. Nat Cell Biol. 2007; 9:847–853. [PubMed: 17558392]

Behr M, Riedel D, Schuh R. The Claudin-Like Megatrachea is Essential in Septate Junctions for the Epithelial Barrier Function in Drosophila. Dev Cell. 2003; 5:611–620. [PubMed: 14536062]

Beitel GJ, Krasnow MA. Genetic Control of Epithelial Tube Size in the Drosophila Tracheal System. Development. 2000; 127:3271–3282. [PubMed: 10887083]

Brand AH, Perrimon N. Raf Acts Downstream of the EGF Receptor to Determine Dorsoventral Polarity during Drosophila Oogenesis. Genes Dev. 1994; 8:629–639. [PubMed: 7926754]

Cela C, Llimargas M. Egfr is Essential for Maintaining Epithelial Integrity during Tracheal Remodelling in Drosophila. Development. 2006; 133:3115–3125. [PubMed: 16831830]

Chen CK, Kuhnlein RP, Eulenberg KG, Vincent S, Affolter M, Schuh R. The Transcription Factors KNIRPS and KNIRPS RELATED Control Cell Migration and Branch Morphogenesis during Drosophila Tracheal Development. Development. 1998; 125:4959–68. [PubMed: 9811580]

Cho NK, Keyes L, Johnson E, Heller J, Ryner L, Karim F, Krasnow MA. Developmental Control of Blood Cell Migration by the Drosophila VEGF Pathway. Cell. 2002; 108:865–876. [PubMed: 11955438]

Devine WP, Lubarsky B, Shaw K, Luschnig S, Messina L, Krasnow MA. Requirement for Chitin Biosynthesis in Epithelial Tube Morphogenesis. Proc Natl Acad Sci U S A. 2005; 102:17014–17019. [PubMed: 16287975]

Ghabrial AS, Levi BP, Krasnow MA. A Systematic Screen for Tube Morphogenesis and Branching Genes in the Drosophila Tracheal System. PLoS Genet. 2011; 7:e1002087. [PubMed: 21750678]

Glazer L, Shilo BZ. The Drosophila FGF-R Homolog is Expressed in the Embryonic Tracheal System and Appears to be Required for Directed Tracheal Cell Extension. Genes Dev. 1991; 5:697–705. [PubMed: 1849109]

Heldin CH, Miyazono K, ten Dijke P. TGF-Beta Signalling from Cell Membrane to Nucleus through SMAD Proteins. Nature. 1997; 390:465–471. [PubMed: 9393997]

Herz HM, Woodfield SE, Chen Z, Bolduc C, Bergmann A. Common and Distinct Genetic Properties of ESCRT-II Components in Drosophila. PLoS One. 2009; 4:e4165. [PubMed: 19132102]

Horowitz A, Simons M. Branching Morphogenesis. Circ Res. 2008; 103:784–795. [PubMed: 18845818]

Imam F, Sutherland D, Huang W, Krasnow MA. Stumps, a Drosophila Gene Required for Fibroblast Growth Factor (FGF)-Directed Migrations of Tracheal and Mesodermal Cells. Genetics. 1999; 152:307–318. [PubMed: 10224263]

Jayaram SA, Senti KA, Tiklova K, Tsarouhas V, Hemphala J, Samakovlis C. COPI Vesicle Transport is a Common Requirement for Tube Expansion in Drosophila. PLoS One. 2008; 3:e1964. [PubMed: 18398480]

Jazwinska A, Affolter M. A Family of Genes Encoding Zona Pellucida (ZP) Domain Proteins is Expressed in various Epithelial Tissues during Drosophila Embryogenesis. Gene Expr Patterns. 2004; 4:413–421. [PubMed: 15183308]

Jeon M, Scott MP, Zinn K. Interactions between Type III Receptor Tyrosine Phosphatases and Growth Factor Receptor Tyrosine Kinases Regulate Tracheal Tube Formation in Drosophila. Biol Open. 2012; 1:548–558. [PubMed: 23213447]

Jeon M, Zinn K. Receptor Tyrosine Phosphatases Control Tracheal Tube Geometries through Negative Regulation of Egfr Signaling. Development. 2009; 136:3121–3129. [PubMed: 19675131]

Jeon M, Nguyen H, Bahri S, Zinn K. Redundancy and Compensation in Axon Guidance: Genetic Analysis of the Drosophila Ptp10D/Ptp4E Receptor Tyrosine Phosphatase Subfamily. Neural Dev. 2008; 3 3-8104-3-3.

Jiang L, Pearson JC, Crews ST. Diverse Modes of Drosophila Tracheal Fusion Cell Transcriptional Regulation. Mech Dev. 2010

Jiang L, Rogers SL, Crews ST. The Drosophila Dead End Arf-like3 GTPase Controls Vesicle Trafficking during Tracheal Fusion Cell Morphogenesis. Dev Biol. 2007; 311:487–499. [PubMed: 17919535]

Jiang L, Crews ST. The Drosophila Dysfusion Basic Helix-Loop-Helix (bHLH)-PAS Gene Controls Tracheal Fusion and Levels of the Trachealess bHLH-PAS Protein. Mol Cell Biol. 2003; 23:5625–5637. [PubMed: 12897136]

Johndrow JE, Magie CR, Parkhurst SM. Rho GTPase Function in Flies: Insights from a Developmental and Organismal Perspective. Biochem Cell Biol. 2004; 82:643–657. [PubMed: 15674432]

Jones TA, Nikolova LS, Schjelderup A, Metzstein MM. Exocyst-Mediated Membrane Trafficking is Required for Branch Outgrowth in Drosophila Tracheal Terminal Cells. Dev Biol. 2014; 390:41–50. [PubMed: 24607370]

Kamiya Y, Miyazono K, Miyazawa K. Specificity of the Inhibitory Effects of Dad on TGF-Beta Family Type I Receptors, Thickveins, Saxophone, and Baboon in Drosophila. FEBS Lett. 2008; 582:2496–2500. [PubMed: 18588885]

Klambt C, Glazer L, Shilo BZ. Breathless, a Drosophila FGF Receptor Homolog, is Essential for Migration of Tracheal and Specific Midline Glial Cells. Genes Dev. 1992; 6:1668–1678. [PubMed: 1325393]

Lamb RS, Ward RE, Schweizer L, Fehon RG. Drosophila Coracle, a Member of the Protein 4.1 Superfamily, has Essential Structural Functions in the Septate Junctions and Developmental Functions in Embryonic and Adult Epithelial Cells. Mol Biol Cell. 1998; 9:3505–3519. [PubMed: 9843584]

Laprise P, Paul SM, Boulanger J, Robbins RM, Beitel GJ, Tepass U. Epithelial Polarity Proteins Regulate Drosophila Tracheal Tube Size in Parallel to the Luminal Matrix Pathway. Curr Biol. 2010; 20:55–61. [PubMed: 20022244]

Lee S, Kolodziej PA. The Plakin Short Stop and the RhoA GTPase are Required for E-Cadherin-Dependent Apical Surface Remodeling during Tracheal Tube Fusion. Development. 2002; 129:1509–20. [PubMed: 11880359]

Li BX, Satoh AK, Ready DF. Myosin V, Rab11, and dRip11 Direct Apical Secretion and Cellular Morphogenesis in Developing Drosophila Photoreceptors. J Cell Biol. 2007; 177:659–669. [PubMed: 17517962]

Llimargas M, Strigini M, Katidou M, Karagogeos D, Casanova J. Lachesin is a Component of a Septate Junction-Based Mechanism that Controls Tube Size and Epithelial Integrity in the Drosophila Tracheal System. Development. 2004; 131:181–190. [PubMed: 14681183]

Llimargas M. Wingless and its Signalling Pathway have Common and Separable Functions during Tracheal Development. Development. 2000; 127:4407–4417. [PubMed: 11003840]

Llimargas M, Casanova J. EGF Signalling Regulates Cell Invagination as Well as Cell Migration during Formation of Tracheal System in Drosophila. Dev Genes Evol. 1999; 209:174–179. [PubMed: 10079360]

Lu P, Werb Z. Patterning Mechanisms of Branched Organs. Science. 2008; 322:1506–1509. [PubMed: 19056977]

Lubarsky B, Krasnow MA. Tube Morphogenesis: Making and Shaping Biological Tubes. Cell. 2003; 112:19–28. [PubMed: 12526790]

Luschnig S, Batz T, Armbruster K, Krasnow MA. Serpentine and Vermiform Encode Matrix Proteins with Chitin Binding and Deacetylation Domains that Limit Tracheal Tube Length in Drosophila. Curr Biol. 2006; 16:186–194. [PubMed: 16431371]

Matozaki T, Murata Y, Mori M, Kotani T, Okazawa H, Ohnishi H. Expression, Localization, and Biological Function of the R3 Subtype of Receptor-Type Protein Tyrosine Phosphatases in Mammals. Cell Signal. 2010; 22:1811–1817. [PubMed: 20633639]

Moussian B, Tang E, Tonning A, Helms S, Schwarz H, Nusslein-Volhard C, Uv AE. Drosophila Knickkopf and Retroactive are Needed for Epithelial Tube Growth and Cuticle Differentiation through their Specific Requirement for Chitin Filament Organization. Development. 2006; 133:163–171. [PubMed: 16339194]

Moyer KE, Jacobs JR. Varicose: A MAGUK Required for the Maturation and Function of Drosophila Septate Junctions. BMC Dev Biol. 2008; 8:99. [PubMed: 18847477]

Myat MM, Lightfoot H, Wang P, Andrew DJ. A Molecular Link between FGF and Dpp Signaling in Branch-Specific Migration of the Drosophila Trachea. Dev Biol. 2005; 281:38–52. [PubMed: 15848387]

Norum M, Tang E, Chavoshi T, Schwarz H, Linke D, Uv A, Moussian B. Trafficking through COPII Stabilises Cell Polarity and Drives Secretion during Drosophila Epidermal Differentiation. PLoS One. 2010; 5:e10802. [PubMed: 20520821]

Ohshiro T, Emori Y, Saigo K. Ligand-Dependent Activation of Breathless FGF Receptor Gene in Drosophila Developing Trachea. Mech Dev. 2002; 114:3. [PubMed: 12175485]

Patel NH, Snow PM, Goodman CS. Characterization and Cloning of Fasciclin III: A Glycoprotein Expressed on a Subset of Neurons and Axon Pathways in Drosophila. Cell. 1987; 48:975–988. [PubMed: 3548998]

Paul SM, Ternet M, Salvaterra PM, Beitel GJ. The Na+/K+ ATPase is Reired for Septate Junction Function and Epithelial Tube-Size Control in the Drosophila Tracheal System. Development. 2003; 130:4963–4974. [PubMed: 12930776]

Reich A, Sapir A, Shilo B. Sprouty is a General Inhibitor of Receptor Tyrosine Kinase Signaling. Development. 1999; 126:4139–4147. [PubMed: 10457022]

Ribeiro C, Neumann M, Affolter M. Genetic Control of Cell Intercalation during Tracheal Morphogenesis in Drosophila. Curr Biol. 2004; 14:2197–2207. [PubMed: 15620646]

Roman BL, Pham VN, Lawson ND, Kulik M, Childs S, Lekven AC, Garrity DM, Moon RT, Fishman MC, Lechleider RJ, Weinstein BM. Disruption of acvrl1 Increases Endothelial Cell Number in Zebrafish Cranial Vessels. Development. 2002; 129:3009–3019. [PubMed: 12050147]

Samakovlis C, Hacohen N, Manning G, Sutherland D, Guillemin K, Krasnow MA. Development of the Drosophila Tracheal System Occurs by a Series of Morphologically Distinct but Genetically Coupled Branching Events. Development. 1996; 122:1395–1407. [PubMed: 8625828]

Schiller MR. Coupling Receptor Tyrosine Kinases to Rho GTPases--GEFs what's the Link. Cell Signal. 2006; 18:1834–1843. [PubMed: 16725310]

Scholz H, Deatrick J, Klaes A, Klambt C. Genetic Dissection of Pointed, a Drosophila Gene Encoding Two ETS-Related Proteins. Genetics. 1993; 135:455–468. [PubMed: 8244007]

Schottenfeld-Roames J, Ghabrial AS. Whacked and Rab35 Polarize Dynein-Motor-Complex-Dependent Seamless Tube Growth. Nat Cell Biol. 2012; 14:386–393. [PubMed: 22407366]

Shi Y. Structural Insights on Smad Function in TGFbeta Signaling. Bioessays. 2001; 23:223–232. [PubMed: 11223879]

Song Y, Eng M, Ghabrial AS. Focal Defects in Single-Celled Tubes Mutant for Cerebral Cavernous Malformation 3, GCKIII, Or NSF2. Dev Cell. 2013; 25:507–519. [PubMed: 23763949]

Tanaka-Matakatsu M, Uemura T, Oda H, Takeichi M, Hayashi S. Cadherin-Mediated Cell Adhesion and Cell Motility in Drosophila Trachea Regulated by the Transcription Factor Escargot. Development. 1996; 122:3697–705. [PubMed: 9012491]

Tonks NK. Protein Tyrosine Phosphatases: From Genes, to Function, to Disease. Nat Rev Mol Cell Biol. 2006; 7:833–846. [PubMed: 17057753]

Tsuneizumi K, Nakayama T, Kamoshida Y, Kornberg TB, Christian JL, Tabata T. Daughters Against Dpp Modulates Dpp Organizing Activity in Drosophila Wing Development. Nature. 1997; 389:627–631. [PubMed: 9335506]

Vincent S, Ruberte E, Grieder NC, Chen CK, Haerry T, Schuh R, Affolter M. DPP Controls Tracheal Cell Migration Along the Dorsoventral Body Axis of the Drosophila Embryo. Development. 1997; 124:2741–50. [PubMed: 9226445]

Ward MP, Mosher JT, Crews ST. Regulation of bHLH-PAS Protein Subcellular Localization during Drosophila Embryogenesis. Development. 1998; 125:1599–1608. [PubMed: 9521898]

Wilk R, Weizman I, Glazer L, Shilo B. Trachealess Encodes a bHLH-PAS Protein and is a Master Regulator Gene in the Drosophila Tracheal System. Genes Dev. 1996; 10:93–102. [PubMed: 8557198]

Wodarz A, Hinz U, Engelbert M, Knust E. Expression of Crumbs Confers Apical Character on Plasma Membrane Domains of Ectodermal Epithelia of Drosophila. Cell. 1995; 82:67–76. [PubMed: 7606787]

Wu VM, Schulte J, Hirschi A, Tepass U, Beitel GJ. Sinuous is a Drosophila Claudin Required for Septate Junction Organization and Epithelial Tube Size Control. J Cell Biol. 2004; 164:313–323. [PubMed: 14734539]

Zhang L, Ward RE 4th. Uninflatable Encodes a Novel Ectodermal Apical Surface Protein Required for Tracheal Inflation in Drosophila. Dev Biol. 2009; 336:201–212. [PubMed: 19818339]

Highlights

- Novel Smad protein Expansion regulates tube diameter in the *Drosophila* trachea.
- Expansion does not function as a typical Smad to regulate TGF-β signaling pathway.
- Expansion regulates Receptor Tyrosine Kinase pathway to control tube- size.

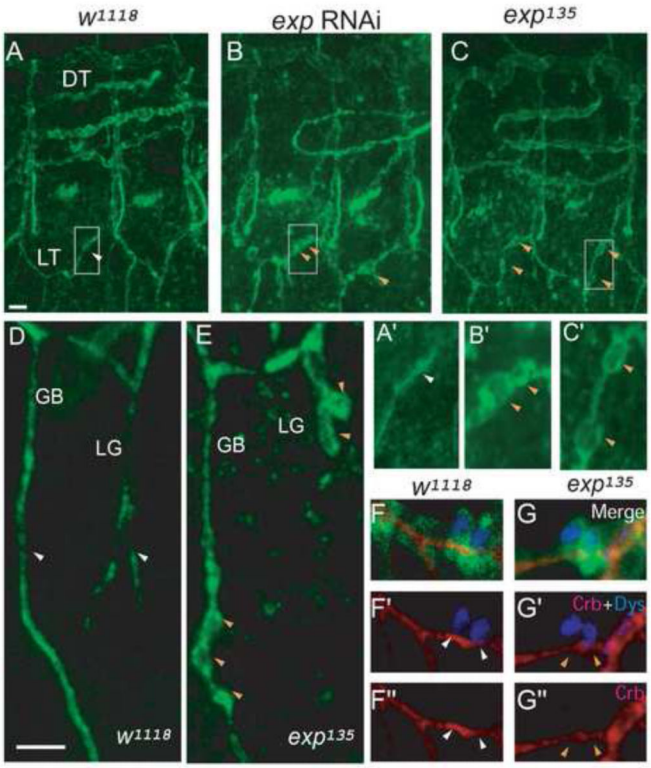

Fig. 1. *exp* mutants develop bubble-like cysts

Stage 16 wild type w^{1118}, *exp* RNAi, and exp^{135} mutant embryos were immunostained for the apical membrane marker Crb. Three hemisegments (5-7) are shown, with anterior to the left and dorsal up. (A) Crb outlines the apical membrane, appearing as a line (white arrowhead) in wild type unicellular LT branches. Enlarged area is indicated in A'. (B) LT branches have cysts (orange arrowheads) outlined by Crb in *exp* RNAi embryos. Enlarged area is indicated in B'. (C) Similar cysts (orange arrowheads) also develop in exp^{135} mutants embryos. Enlarged area is indicated in C'. (D) Crb outlines unicellular branch GB and intracellular branch LG. Both of them appear as a line (white arrowheads) in wild type embryos. (E) Both GB and LG have cysts (orange arrowheads) in exp^{135} mutants. Stage 16 w^{1118} and exp^{135} embryos carrying *btl-Gal4 mCD8-GFP* were immunostained for apical membrane Crb (red) and fusion cell nuclear marker Dys (blue) to analyze the fusion of LT branches. mCD8-GFP (green) outlines the cell boundary. (F-F") The fused LT branch (shown by white arrowheads) outlined by Crb (red) along with two fusion cells (blue) appears a single line in w^{1118} embryo. (G-G") The fused LT branch (shown by orange arrowheads) has normal wild type appearance without cysts in exp^{135} mutants. The white line in A represents 10 μm in A, B, and C. The white line in D represents 5 μm in the rest of the panels.

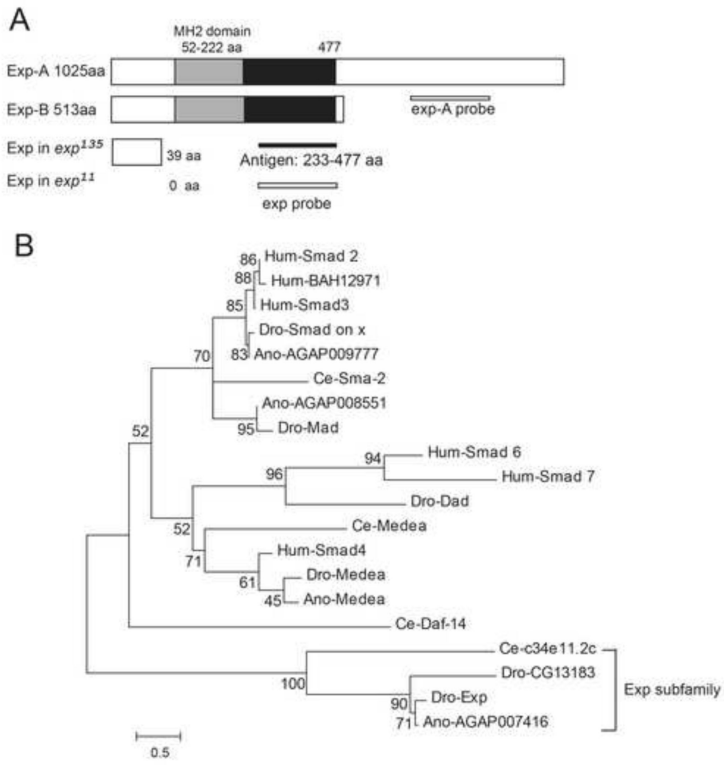

Fig. 2. Identity of the *Drosophila exp* gene

(A) Exp is a Smad-like protein containing an MH2 domain (grey box). Exp exists in two isoforms: Exp-A (1025 aa) and Exp-B (513 aa). The first 477 amino acids (grey and black boxes), including the MH2 domain (55-222 aa), are identical in both isoforms. An anti-Exp antibody that recognizes both isoforms was generated against an Exp fragment containing amino acids 233-477 (black line). The same region was used to generate an *exp* probe that recognizes both isoforms. The region that was used to generate a specific *exp-A* probe that recognizes *exp-A* is shown. (B) Exp belongs to a distinct subfamily of Smad-like proteins. The alignment is represented by a phylogram generated using the neighbor-joining method. The tree demonstrated that Dro-Exp, Ano-AGAP007416, Dro-CG13183, and Ce-C34E11.2C represent a distinct, evolutionarily conserved subfamily of Smad proteins that we named the Exp subfamily. Protein sequences of the MH2 domains of Smad proteins were compared and aligned using ClustalW. The scale represents the fraction of nonidentical amino acid residues along each branch. The species designation precedes each protein acronym (Dro, *Drosophila melanogaster*; Ano, *Anopheles gambiae*; Ce, *Caenorhabditis elegans*; Hum, human).

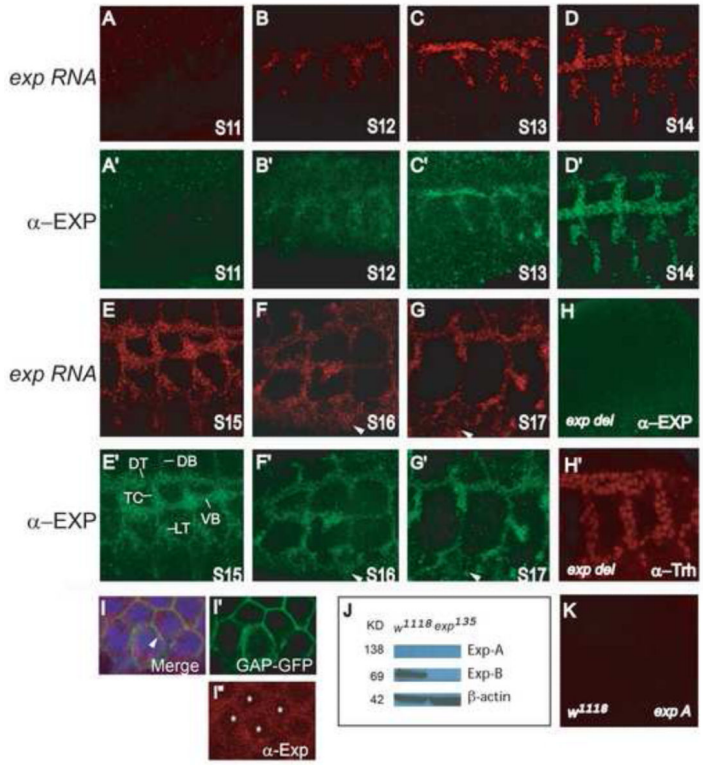

Fig. 3. Exp is localized throughout the cytoplasm of all tracheal cells

The localization of *exp* RNA and Exp protein was analyzed by fluorescence *in situ* hybridization (FISH) to an *exp* RNA probe and followed by immunostaining with anti-Exp antisera using whole mount wild type embryos. The *exp* probe and the anti-Exp antisera recognize both isoforms. Sagittal views of tracheal segments 3-7 are shown, anterior is to the left and dorsal is up. Dorsal trunk (DT), transverse connective (TC), lateral trunk (LT), visceral branch (VB), and dorsal branch (DB) were labeled. (A-G) *exp* RNA is expressed throughout the trachea from stages 12-17, but not at stage 11. Additionally, *exp* RNA is also observed in epidermal cells at stage 16 and 17 (arrowheads). (A'-G') The Exp protein has the exact same expression pattern as *exp* RNA. It is expressed in all tracheal cells from stages 12-17, but not at stage 11. The Exp protein is also observed in epidermal cells at later stages (arrowheads). To visualize intracellular localization of Exp, wild type embryos containing *btl-Gal4 UAS-GAP-GFP* were co-immunostained with anti-Exp (red in I, I"), anti-GFP that stains the cell membrane marker GAP-GFP (green in I, I'), and anti-Trh that stains tracheal nuclei (blue in I), shown in DT cells. Exp is clearly localized throughout the cytoplasm (red in I) and also partially overlaps with the membrane (yellow in I; arrowhead). (H) Exp protein is not detected in homozygous *Df(2R)BSC879* embryos, which delete the entire *exp* gene locus and several other genes, even though tracheal cells are present (labeled by Trh (red) in H'). (J) The 69KD Exp-B isoform is detected in cell lysate from wild type but not exp^{135} mutant embryos by Western blot using anti-Exp antisera. However, the 139KD Exp-A is not detected in wild type. (K) *exp-A* RNA is not detected by FISH using an *exp-A* RNA probe that only recognizes the *exp-A* isoform.

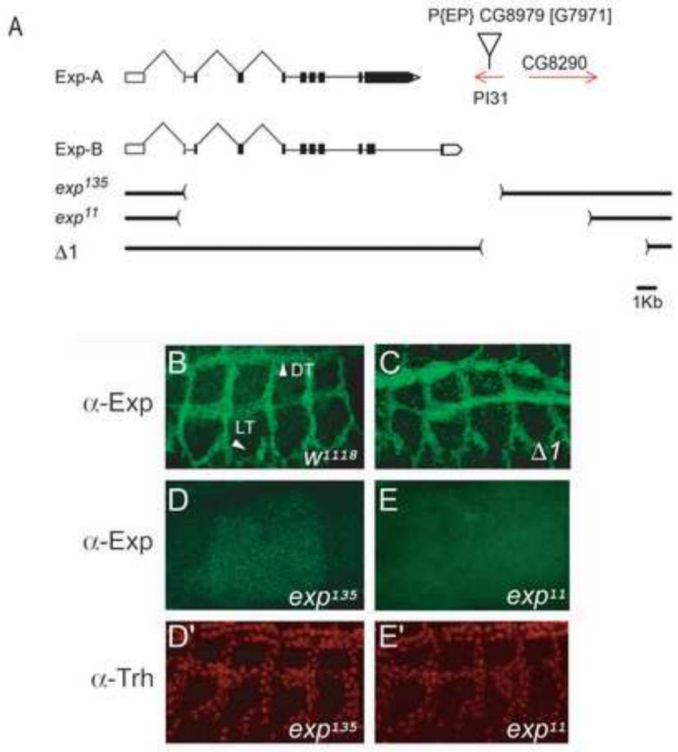

Fig. 4. Analysis of *exp*> null mutants

(A) Genomic structure of the *exp* locus. The schematic diagram indicates the structure of the mRNA transcripts. Boxes indicate the exons, connecting lines indicate the introns, protein coding sequences in the exons are filled with black, and untranslated regions are left white. Red lines with arrowheads indicate the two neighboring genes, *PI31* and *CG8290*. Brackets below the gene schematics indicate the region deleted in exp^{135}, exp^{11}, and Δ*1*. represents the P element insertion site. (B) Exp protein (green) was localized to all tracheal cells in w^{1118} control embryos. (C) Exp protein was present in all tracheal cells in Δ*1* mutant embryos that lack both *PI31* and *CG8290*, indicating that Δ*1* was not mutant for *exp*. (D-E) Exp protein was not detected in exp^{135} and exp^{11} homozygous mutant embryos. (D'-E') Trh staining (red) revealed the presence of tracheal cells in both mutants.

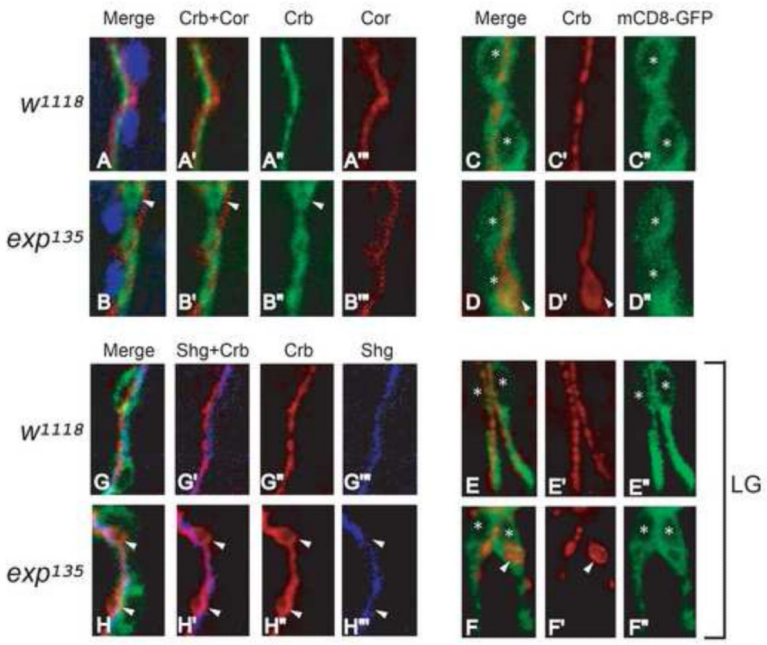

Fig. 5. Cysts are apical compartments within the cell boundary in unicellular and intracellular branches in *exp* mutants

(A-B"') Stage 15 w^{1118} and exp^{135} embryos were immunostained with the apical membrane marker Crb, basolateral membrane marker Cor, and tracheal nuclei marker Trh, to visualize apical-basal polarity in wild type and exp^{135} mutant embryos. Unicellular branch GBs were shown. Both Crb (green) and Cor (red) appear as single lines without overlapping in wild type embryos (A-A"'). Similarly, cysts outlined by Crb do not overlap with Cor in exp^{135} mutant embryos (B-B"'), indicating that cysts are apical compartments. (G-H"') Stage 15 w^{1118} and exp^{135} embryos containing *btl-Gal4 mCD8-GFP* that outlines the cell boundary were immunostained for Crb and the AJ marker Shg. Shg (blue) labels a line of autocellular junctions along the apical membrane (red) in wild type GB (G-G"'). Similarly, Shg (blue) labels a line of autocellular junctions despite cyst (red) formation in exp^{135} embryos, suggesting that cysts are part of the extracellular lumen in unicellular branches (HH"'). (C-F") Stage 15 w^{1118} and exp^{135} embryos containing *btl-Gal4 mCD8-GFP* were immunostained for Crb and the cell membrane marker GFP. In wild type embryos, Crb (red) appears as a line within the cell boundary marked by mCD8-GFP (green) in unicellular branch GB (C-C") and intracellular branch LG (E-E"). Similarly in exp^{135} mutant embryos, cysts (white arrowheads) in GB (D-D") and LG (F-F") are also within the mCD8-GFP labeled cell boundary. Nuclei were labeled by asterisks.

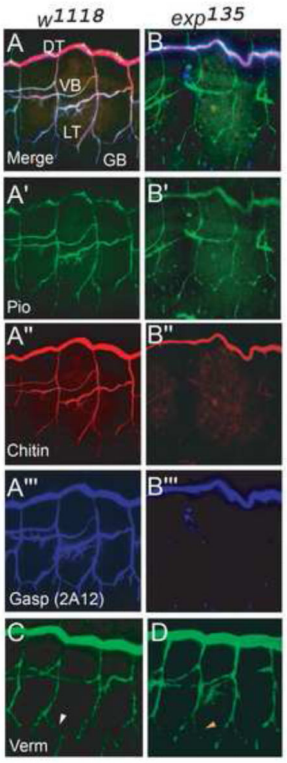

Fig. 6. Luminal Gasp (2A12) and chitin fail to accumulate in unicellular and intracellular branches that develop cysts

(A-B”’) Stage 16 wild type w^{1118} and exp^{135} embryos were stained with anti-Gasp (MAb 2A12) (blue), chitin probe (red), and anti-Piopio (green). (A-A”’) In w^{1118} embryos, Gasp (2A12), chitin, and Piopio accumulate in the lumen of all branches. (B-B”’) In exp^{135} mutant embryos, Piopio accumulates in all branches like in wild type. However, Gasp (2A12) and chitin only accumulate in the lumen of DT but not other branches. (C, D) Similar to wild type embryos, Verm is secreted to the lumen in all branches in exp^{135} mutants. However, in LT, Verm (orange arrowhead) in exp^{135} mutants is slightly weaker compared to wild type LT (white arrowhead).

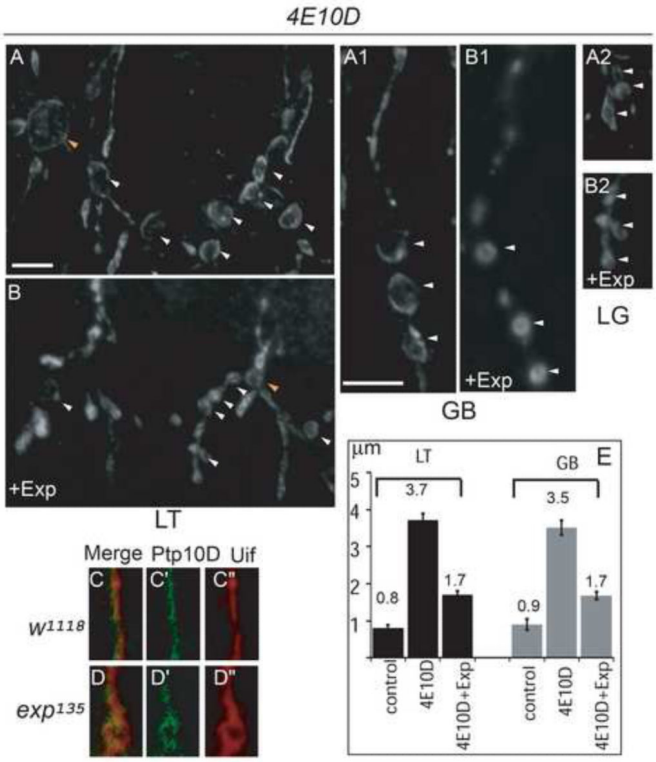

Fig. 7. Exp expression suppresses cyst phenotype in *Ptp4EPtp10D* double mutants, and Exp is not required for the distribution of Ptp10D

Stage 16 embryos were stained with anti-Uif to label the tracheal apical membrane and imaged using confocal microscopy. LT in tracheal segments 5-6 were shown, GB in tracheal segment 6 was shown. (A-B2) Expression of HA-Exp-B in *Ptp4EPtp10D* embryos significantly reduced cyst size in LT (B), GB (B1) and LG (B2) compared to cysts in *Ptp4EPtp10D* embryos (A, A1, A2). In addition, TC/LT branch junction cyst size was also significantly reduced. White arrowheads point to LT and GB cysts and orange arrowheads point to TC/LT junction cysts. Quantification of LT and GB cysts is shown by the bar graph (E). Single GB stained with anti-Ptp10D (green) and the apical membrane marker Uif (red) in wild type (C-C") and exp^{135} mutant embryos (D-D") were shown. Ptp10D (C-C') was localized at the apical membrane labeled with Uif (C") in wild type embryos. Similarly, Ptp10D (D-D') was also localized around cysts outlined with Uif (D"). The white line in B represents 10 µm in A and B. The white line in A1 represents 10 µm in the rest of the panels.

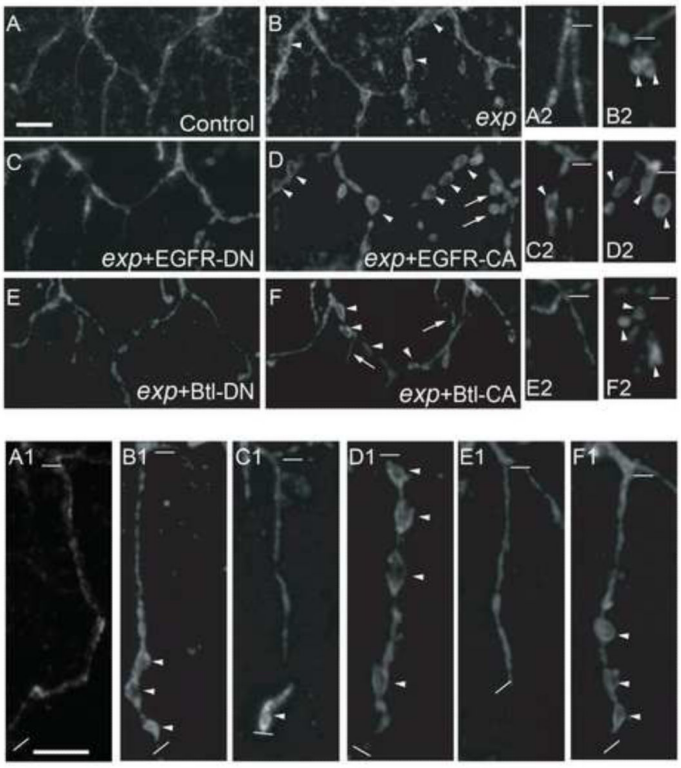

Fig. 8. Effects of dominant negative (DN) and constitutively active (CA) receptor tyrosine kinase (EGFR, Btl) mutants on cyst phenotype in *exp* mutants

Stage 16 embryos were stained with anti-Uif to label the apical membrane. The tracheal specific driver *btl-Gal4* was used to express all mutant UAS-RTK constructs in exp^{135} mutants. EGFR-CA expression in exp^{135} mutants greatly enhanced the cyst phenotype in LT (D), GB (D1), and LG (D2) compared to exp^{135} mutants (B, B1, B2). Extra branching was observed (arrows in D). To a lesser extent, Btl-CA also enhanced the cyst phenotype (F, F1, F2). EGFR-DN significantly reduced cysts in LT (C) and partially suppressed cysts in GB (C1) and LG (C2). Btl-DN dramatically reduced the cyst phenotype in all branches analyzed (E, E1, E2), and almost restored the phenotype to wild type level (A, A1, A2). The thick white line in A represents 10 μm in panels A-F. The thick white line in A1 represents 10 μm in the rest of the panels. The thin white lines indicate the beginning and the end of each GB in A1-F1, and the beginning of LG in A2-F2.

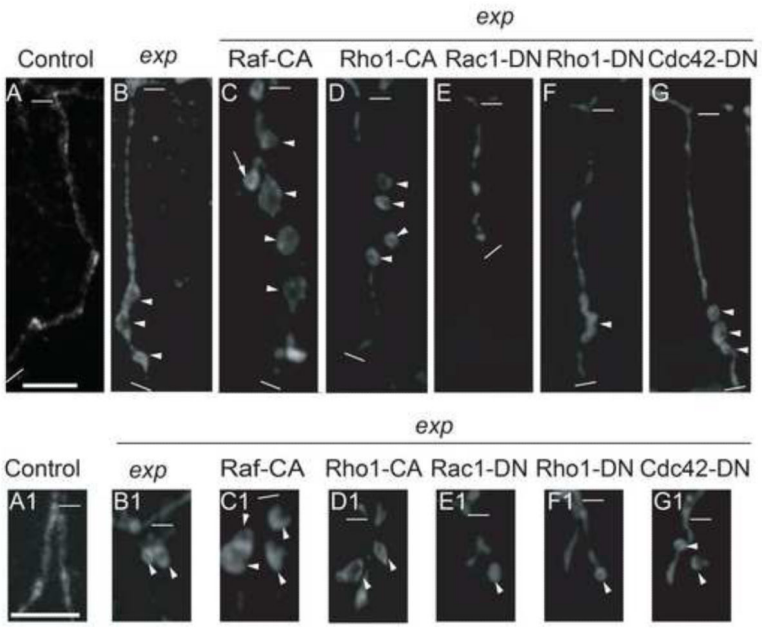

Fig. 9. Effect of Map kinase and Rho pathway mutants on cyst phenotype in *exp* mutants

Stage 16 embryos were stained with anti-Uif to label the apical membrane. The tracheal specific driver *btl-Gal4* was used to express CA or DN constructs in exp^{135} mutants. Images of GB (A-G) and LG (A1-G1) stained with anti-Uif are shown. Strong enhancement of the *exp* phenotype in both GB (C) and LG (C1) was observed with Raf-CA expression. Extra branching was observed (arrow in C). Partial enhancement in GB (D) and LG (D1) was observed by Rho1-CA expression. Strong suppression of the GB cyst phenotype was observed by Rac1-DN (E) and Rho1-DN (F). GB extension defect was observed by Rac1-DN (E). Partial suppression of the LG cyst phenotype was observed by Rac1-DN (E1) and Rho1-DN (F1). No obvious suppression of GB (G) and LG (G1) cysts was observed by Cdc42-DN. The thick white line in A represents 10 μm in panels A-G. The thick white line in A1 represents 10 μm in the rest of panels. The thin white lines indicate the beginning and the end of each GB in A-F, and the beginning of LG in A1-F1.

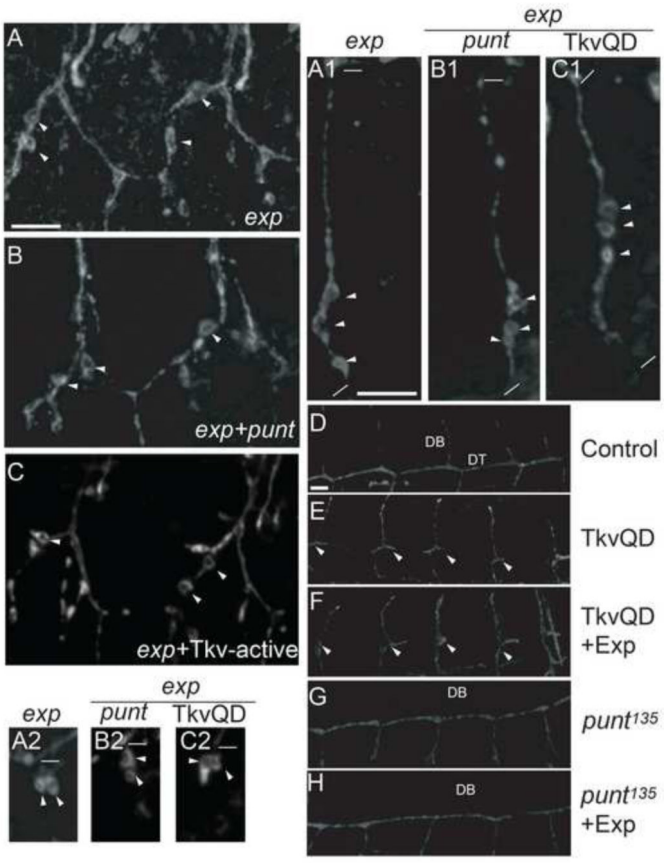

Fig. 10. TGF-β (Dpp) signaling and Exp do not genetically interact

(A-C2) Stage 16 embryos were stained with anti-Uif to label the apical membrane in the trachea. No obvious enhancement or suppression of the cyst phenotype was observed in LT (B), GB (B1), and LG (B2) in *exp punt* double mutant embryos compared to *exp* mutants alone (A, A1, A2). Similarly, enhancing TGF-β signaling by TKV253 QD (TKV-active) expression in an *exp* mutant background using *btl-Gal4* did not change the cyst phenotype in LT (C), GB (C1), and LG (C2). The thick white line in A represents 10 μm in panels A-C. The thick white line in A1 represents 10 μm in A1-C2. The thin white lines indicate the beginning and the end of each GB in A1-C1, and the beginning of LG in A2-C2. (D-H) Stage 15 embryos were stained with anti-Uif to label the apical membrane in the trachea. TkvQD expression in trachea caused DT migration defects (arrowheads) in (E) compared to control (D). Overexpression of both Exp and TkvQD in trachea had similar DT migration defect (F). DB migration defect was observed in $punt^{135}$ mutant embryos (G). Similarly, DB migration defect was still observed when Exp was expressed in $punt^{135}$mutants (H). The thick white line in D represents 10 μm in D-H.